



Karl F. Warnick

Wireless Body Area Network for Heart Attack Detection

Georg Wolgast, Casimir Ehrenborg, Alexander Israelsson, Jakob Helander, Edvard Johansson, and Hampus Månefjord

This article describes a body area network (BAN) for measuring an electrocardiogram (ECG) signal and transmitting it to a smartphone via Bluetooth for data analysis. The BAN uses a specially designed planar inverted F-antenna (PIFA) with a small form factor, realizable with low-fabrication-cost techniques. Furthermore, due to the human body's electrical properties, the antenna was designed to enable surface-wave propagation around the body. The system utilizes the user's own smartphone for data processing, and the built-in communications can be used to raise an alarm if a heart attack is detected. This is managed by an application for Android smartphones that has been developed for this system. The good functionality of the system was confirmed in three real-life user case scenarios.

BACKGROUND

Heart disease is the most common cause of death in the world [1], and the survival rates of heart-related events are directly related to the response time of medical personnel [2]. People experiencing myocardial infarction do not seek medical care, on average, for ~1.5–2 h after symptom onset [3]. By performing a long-term and

EDITOR'S NOTE

This issue's "Education Corner" column features an article by Georg Wolgast, Casimir Ehrenborg, Alexander Israelsson, Jakob Helander, Edvard Johansson, and Hampus Månefjord, who won first prize in the 2015 IEEE Antennas and Propagation Society Student Design Contest. The contest topic was the design of an antenna for a body area network, and the authors describe their entry for the contest, a wireless body area network for heart attack detection. Congratulations to the team on their success in the design contest.

continuous tracking of the ECGs of an individual, myocardial infarction (more commonly known as a *heart attack*) and other fatal heart-related malfunctions may be detected hours before the user would have sought medical treatment.

Figure 1 shows that ECG readings have a distinct ST elevation during a myocardial infarction, and the detection of such an abnormality is one of

the most reliable signs of myocardial infarction [4]. The proposed system is able to detect ST elevations, thus making it feasible for the user's smartphone to activate the built-in global positioning system to obtain the location and instantly alert emergency services. As a significant percentage of the world's population uses smartphones [5], an Android application was chosen to process the data.

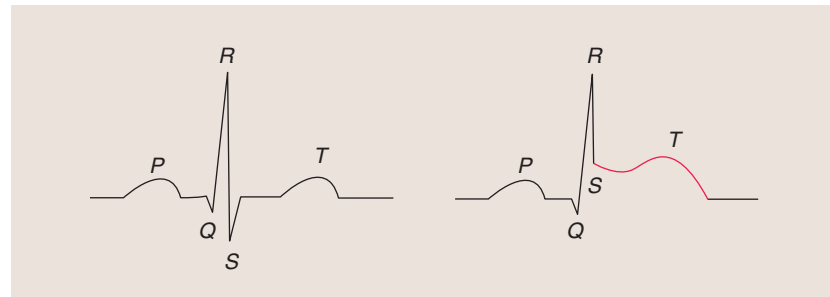


FIGURE 1. A normal ECG signal and an ST elevated signal. The relevant sections are the P wave, the QRS complex, and the T wave. Another important section of the ECG signal for heart disease is the ST segment [4]. The ST segment is the flat isoelectric section of the ECG between the end of the QRS complex and the beginning of the T wave.

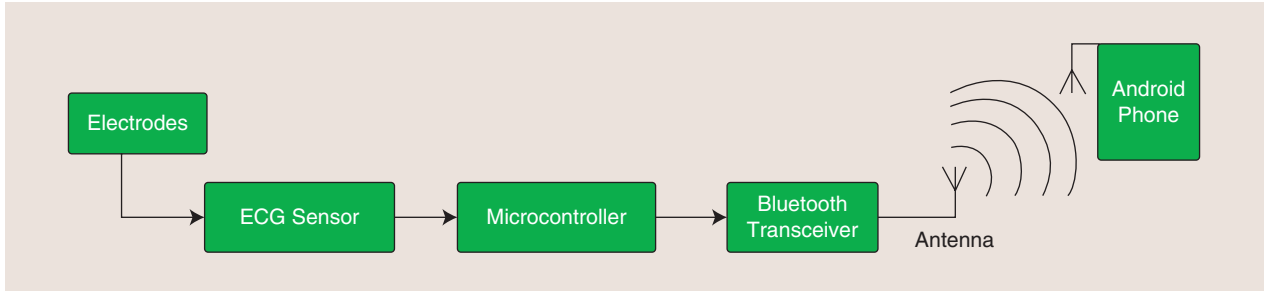


FIGURE 2. A block diagram of the BAN. The antennas are represented by a standard antenna symbol. The physical connections are represented by arrows, and the wireless transmission is represented by concentric half-circles.

Myocardial infarction is caused primarily by blood clotting, and low doses of the common aspirin pill can act as a blood thinner [6]. The proposed system can notify the user to take an aspirin pill to prevent further blood clotting. The ability to immediately self-medicate and the decreased response time can lead to significantly increased survival rates [7].

The proposed system complements some of the systems for heart problem management in use today. Some people with a high risk of heart issues have alarms installed in their homes that are triggered by pressing a button. The proposed system has a similar functionality; however, it is automatic and available outside of the home. Applications are available for people with cardio-pulmonary resuscitation training that will automatically notify the users if there is an emergency situation in their vicinity [8]. Such features could easily be integrated in the proposed system's Android application.

This article gives an overview of the system and a list of materials with assembly and operation examples. Each part of the system is discussed in greater detail. Finally, simulated and measured results are presented to anticipate and validate the performance of the system.

SYSTEM

Figure 2 shows an overview of the proposed system, which consists of an ECG sensor that uses electrodes fastened with adhesive tape to the user's chest to measure an ECG signal. The measurements are sent to a microcontroller, where they are processed and sent to a Bluetooth transceiver. The data are

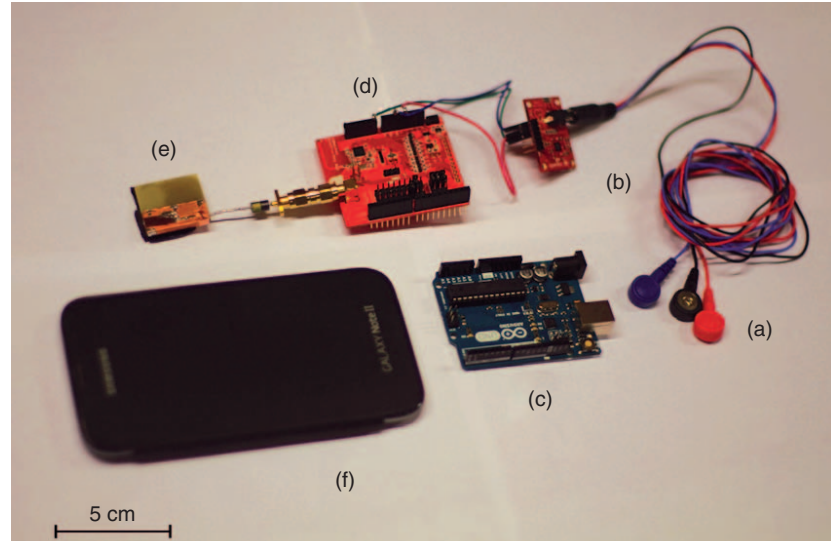


FIGURE 3. The components: (a) electrodes, (b) an ECG sensor, (c) a microcontroller, (d) a Bluetooth transceiver, (e) an antenna, and (f) an Android phone.

broadcast to the user's phone via a PIFA of our own design. They are received and processed in an application that displays the ECG and the received signal strength. Figure 3 shows the components, and Table 1 provides a bill of the materials. The electrodes are connected to the ECG board via standard electrode cables. The microcontroller is connected by a wire to the ECG sensor and attached directly to the transceiver. All of the components, except the antenna and the electrodes, are contained in an assembly box.

When using the system, the electrodes are fastened with adhesive tape to the user's chest, the assembly box is placed in a comfortable position on the user's chest, and the application is downloaded to an Android smartphone and started. Once the sensors are connected, the system is ready to use, as shown in Figure 4.

SENSOR

The sensor solution is composed of three electrodes, two for measurements and one for reference. The electrodes are connected to a board with filters and amplifiers specifically created for ECG signals (an AD8232 single-lead heart rate monitor, SparkFun Electronics, Niwot, Colorado).

The signal is processed by an ATmega328 microcontroller (Atmel, San Jose, California) built into an UNO board (Arduino, Somerville, Massachusetts). This microcontroller was chosen because it has enough space to fit the code for controlling the transceiver and has low power consumption. The analog-to-digital converter has a 10-b resolution, which is enough to sample an ECG [9].

The integrated-circuit Bluetooth low-energy nRF8001 transceiver (Nordic Semiconductor, Oslo,

TABLE 1. A LIST OF MATERIALS.

Description	Name	Retailer	Cost
Electrodes	Plastics One electrode cable	Electrokit (Malmö, Sweden)	US\$6.90
ECG sensor	AD8232 single-lead heart rate monitor	Electrokit	US\$18.64
Microcontroller	Arduino UNO board (ATmega328) revision 3	Electrokit	US\$18.64
Transceiver	RedBearLab Bluetooth 4.0 low-energy shield version 2.1	Electrokit	US\$24.27
Assembly box	Kemo electronic assembly box	Kjell & Company (Malmö, Sweden)	US\$5.21
Battery	Kjell & Company	Kjell & Company	US\$2.31
Antenna	PIFA	Self-made	US\$24
Total cost			US\$100

Norway) has a maximum power output with a nominal value of 0 dBm. It is connected to the UNO board via a Bluetooth 4.0 low-energy shield version 2.1 breakout board (RedBearLab,

Hong Kong). The transceiver communicates with the UNO board using a serial peripheral interface. The transceiver was chosen because it is well documented and has good software

libraries. Figure 5 shows a detailed scheme of the sensor system.

ANDROID APPLICATION

The Android application is made to handle data from the sensor. The application has two modes: one that displays ECG voltage readings and one that shows the signal strength. The modes can be chosen by pressing a button. As the application is launched, it performs a scan for devices and allows the user to select the ECG sensor. The application then receives and interprets data from the sensor and displays it on the screen as a plot. Figure 6 shows an image of the ECG printout.

ANTENNA DESIGN

The goal when designing the antenna was to create a small planar antenna (no larger than 30 mm × 30 mm × 5 mm) with good free-space characteristics that would create surface-wave propagation along the body on which it was placed. To fulfill these specifications, the PIFA design was chosen. A PIFA is a typical antenna that can be much smaller than the customary $\lambda/2$ size [10]. To enable inexpensive and fast manufacturing of the prototype antenna, the design was restricted to concepts realizable by hand and through chemical etching. Thus, all vertical metal lines would have to be placed on the sides of the antenna to allow easy application without the use of advanced machinery.

To fit the feeding cable within the limited volume, the thickness of the substrate layer was limited to 3 mm. The layer

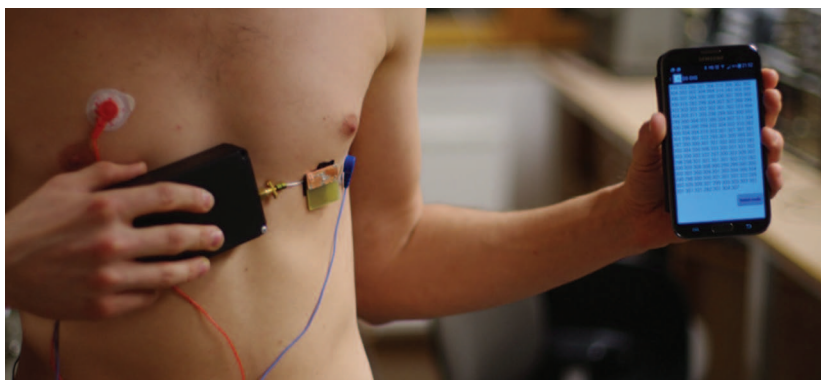


FIGURE 4. The entire BAN. Two electrodes are placed on the chest, and one electrode is placed on the back as a reference. The application can be seen printing out the measured data.

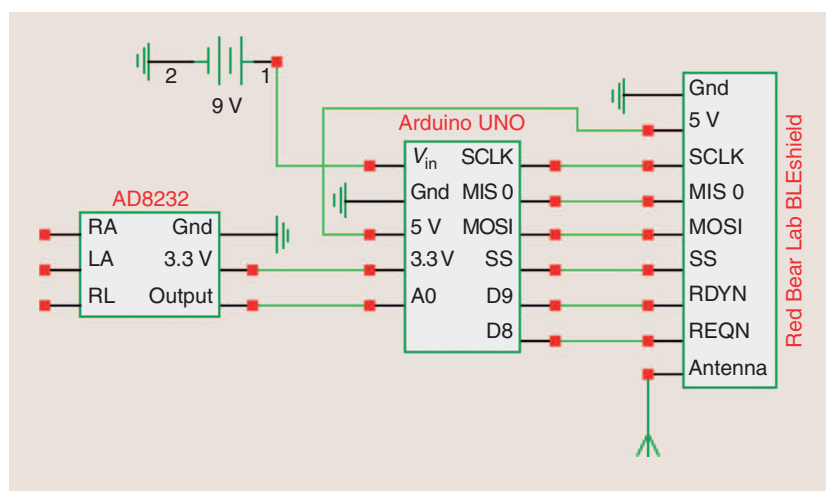


FIGURE 5. A scheme of the sensor system and the wiring. The three electrodes are connected to the right-arm (RA), left-arm (LA), and right-leg (RL) inputs on the left side of the AD8232 single-lead heart rate monitor.



FIGURE 6. A screen capture from the application of an ECG measured with the BAN. The readings strongly resemble a normal ECG signal. The R, S, and T segments are visible and resemble a normal ECG, as shown in Figure 1. The P and Q segments are toned down but can be surmised from the figure.

was constructed by gluing together two 1.5-mm-thick FR-4 laminate plates. The glue used was LOCTITE 431 (Loctite, Düsseldorf, Germany) with a dielectric constant of 2.92 at 10 MHz [11]. The antenna performance was simulated both with and without the glue, and it had no significant effect on the performance, possibly due to the limited thickness of the glue. The plates had copper coating that was removed by chemical etching. The feeding structure and the shortening plate were added using copper tape.

To shield the antenna from the enormous dielectric load of the body,

the ground plane was extended almost to the design-specification limits, 30 mm \times 29.6 mm. Because the shortening strip had to be placed on the side of the structure, the active element was situated on one side of the square. This had the added benefit of launching the radiation pattern away from the shorted side of the antenna (see Figure 7) but meant that the antenna could no longer be freely placed.

To increase the bandwidth of the antenna, it was fed through a wide plate that distributes the current evenly over the active element [12], [13]. In the ground plane, a feeding plate was inserted to increase the reliability of radiation characteristics and ease the manufacturing process. To avoid shortening the antenna through the body, a layer of insulating tape was placed over the exposed feed. Figure 8 shows the dimensions of the antenna, and Figure 9 shows the final antenna design.

SIMULATIONS AND CALCULATIONS

The initial antenna design was simulated in CST Microwave Studio 2014 (Computer Simulation Technology, Darmstadt, Germany). The antenna should be operating at the Bluetooth band (2.440–2.448 GHz) when

mounted on the body, which can be seen as a large dielectric load. Thus, the antenna was mounted during simulation with its grounded side on a large rectangular block of homogeneous dielectric $\epsilon_r = 50$ and $\sigma = 1.7 \text{ S/m}$ [14]. Figure 8 shows the images and measurements of the final antenna design. Figures 7 and 10 show the simulated radiation pattern and return loss, respectively.

Figure 7 presents a comparison of the simulated far-field radiation pattern in free space and with the added dielectric block. The presence of the dielectric block pulls the main lobe down toward its surface, simultaneously making the pattern more directional toward 90°, away from the PIFA's shorted side.

Figure 10 shows that the resonance frequency of the antenna increases as the dielectric load is added. The resonance deepens and thus increases the 10-dB bandwidth of the antenna. This effect occurs as the added losses decrease the Q factor of the system [15]. The simulated 10-dB bandwidths were 105 and 143 MHz for free space and on body, respectively, thus covering the entire Bluetooth band.

The minimum requirement for Bluetooth receiver sensitivity is -70 dBm [16]. To estimate the required free-space

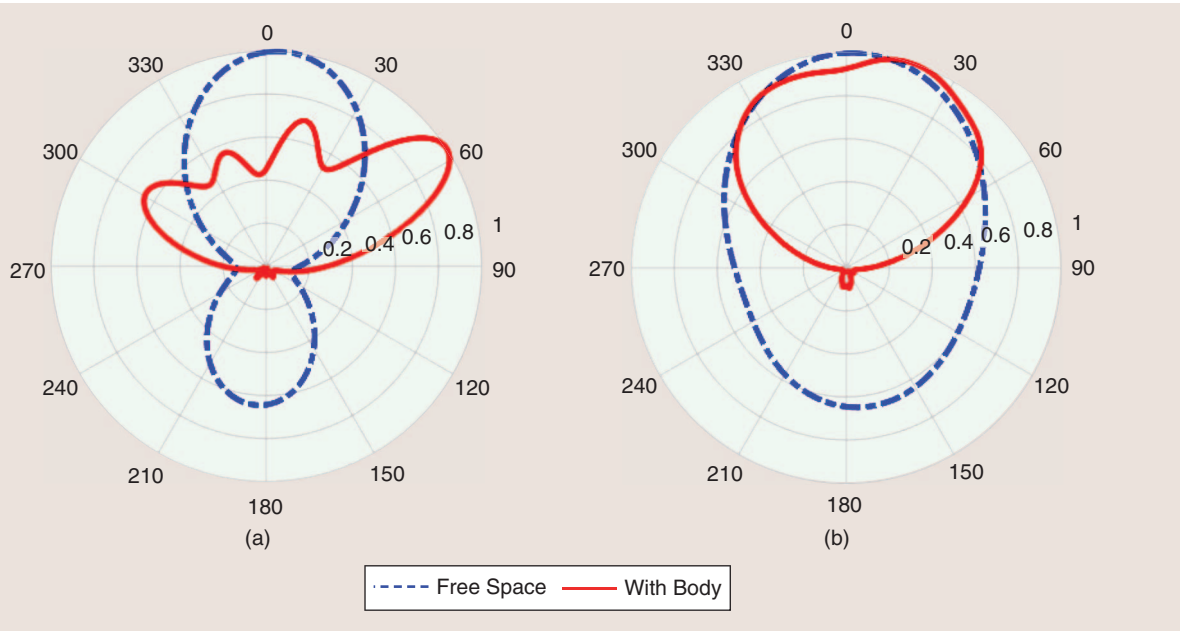


FIGURE 7. The far-field radiation patterns in (a) an E plane and (b) an H plane in normalized linear scale from performed simulations with and without a dielectric block as the background material. 0° is the normal direction away from the block. The shorted side of the PIFA faces 270°.

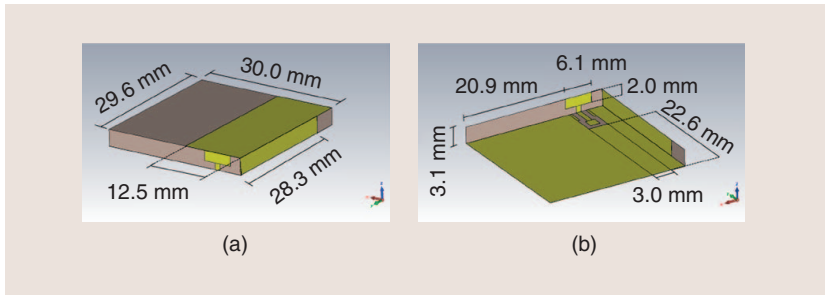


FIGURE 8. The CST model of the simulated antenna with the measurements specified. The coaxial cable adds 1.9 mm to the height, making the total height 5 mm. (a) Top view. (b) Bottom view.

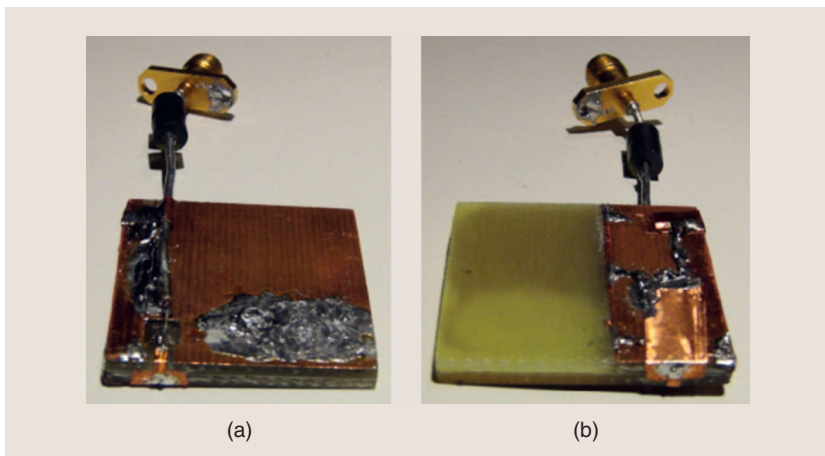


FIGURE 9. The antenna displaying (a) the ground plane and (b) the active element.

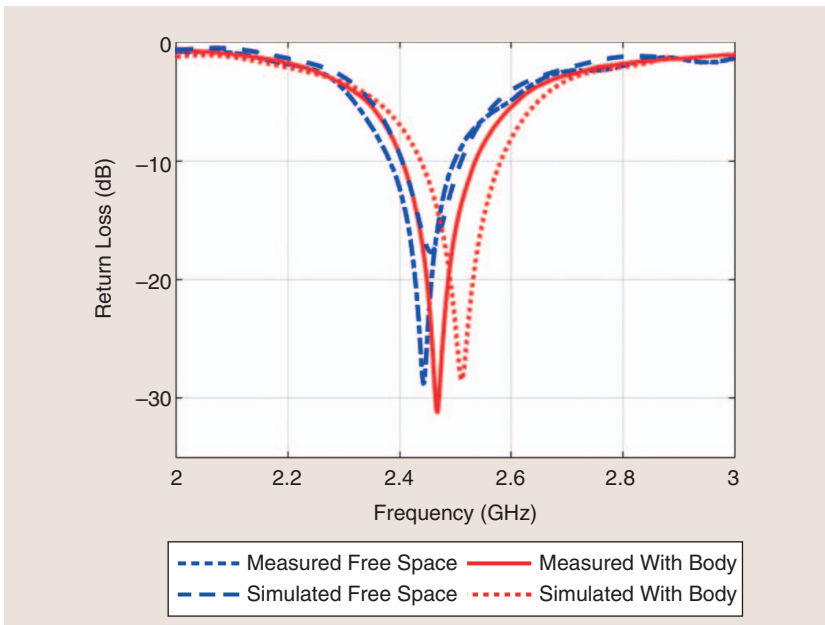


FIGURE 10. The simulated and measured return losses of the antenna. During simulation, the body was modeled as a dielectric slab with the dimensions 30 mm \times 400 mm \times 400 mm. The simulated 10-dB bandwidths were 105 MHz (4.3%) and 143 MHz (5.7%) for free space and on body, respectively. The measured 10-dB bandwidths were 116 MHz (4.7%) and 132 MHz (5.4%) for free space and on body, respectively.

TABLE 2. THE ESTIMATED LINK BUDGET FOR THE FREE-SPACE TRANSMISSION.

Antenna gain	-1 dBi
Loss in free space at 1 m	-40 dB
Receiver gain	-5.3 dBi
Total loss	-46.3 dBm

signal strength, the Friis transmission equation can be used for given values of received and transmitted gains

$$\frac{P_r}{P_t} = G_t G_r \left(\frac{\lambda}{4\pi R} \right)^2, \quad (1)$$

where P_r is the power input of the receiving antenna, P_t is the power output of the transmitting antenna, G_t is the antenna gain of the transmitting antenna, G_r is the antenna gain of the receiving antenna, λ is the wavelength, and R is the distance between antennas. G_t was simulated to be -1 dBi, and G_r was approximated to be -5.3 dBi based on the antenna gain for the Nexus 4 E960 smartphone (LG Electronics, Seoul, South Korea) [17]. For a distance of 1 m, the total loss was estimated to -46.3 dBm, as shown in Table 2, indicating that the requirement of the received signal strength should be easily met in free space.

When modeling at Bluetooth frequencies (i.e., ~2.4 GHz), the electric parameters of the body are approximately $\epsilon_r = 50$ and $\sigma = 1.7$ S/m [14]. This results in >120-dB attenuation for propagation through the body [14]. Thus, it is untenable to consider a solution that sends radiation through the body.

However, as demonstrated in [14], propagation to the other side of the body is still possible without the use of indirect scattering and has been experimentally proven. This occurs through induction of a creeping wave, which propagates along the body's surface. This type of wave also attenuates quickly but is dependent on polarization [14]. Radiation polarized tangentially to the body's surface will decay at a much greater rate than radiation polarized in the normal direction.

Because the PIFA transmits both vertically and horizontally polarized

radiation, it is capable of inducing creeping waves that can propagate longer distances. In [14], the calculation was carried out for a transmitter and a receiver placed on opposite sides of the user's waist; the resulting attenuation was then ~ 50 – 60 dB. For the application of this article, the considered path stretches from the middle of the torso to the back pocket of the user. Thus, attenuation will be greater due to a longer propagation path and irregular geometry. Table 3 provides an approximate link budget for surface waves reaching the back pocket of the user based on the values in [14]. The maximum transmitting-antenna gain was simulated to -1.5 dBi, and the receiving-antenna gain was approximated to -5.3 dBi.

Consequently, the antenna was chosen based on its ability to generate surface waves. The simulations indicate, as shown in Figure 8, that the proposed design radiates along the body. Hence, the proposed PIFA should be more than capable of producing the radiation needed for creeping-wave propagation. It is worth noting that, according to [14], the efficiency drops from -0.8 dBi in free space to -6.1 dBi on the body surface due to a large part of the near-field being concentrated inside the body.

TABLE 3. THE ESTIMATED LINK BUDGET FOR A CREEPING-WAVE TRANSMISSION OF ~ 1 m.

Antenna gain	-1.5 dBi
Loss on surface	-60 dB
Receiver gain	-5.3 dBi
Total loss	-66.8 dBm

TABLE 4. THE SIGNAL STRENGTH MEASURED WITH THE ANDROID APPLICATION.

1-m free space	-52 dBm
Front pocket	-55 dBm
Back pocket	-68 dBm

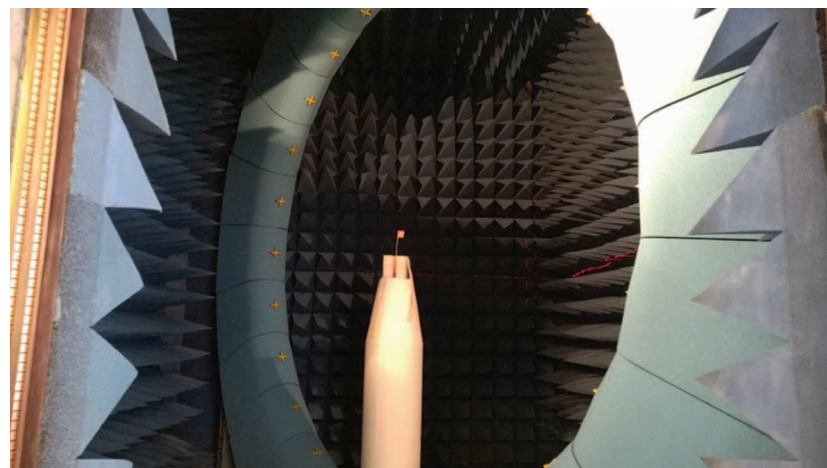


FIGURE 11. The Satimo Stargate 24 measuring chamber at Lite-On Mobile Mechanical in Lund, Sweden. The antenna is mounted on the test station.

TESTING

The bandwidth, return loss, efficiency, signal strength, and far-field radiation of the antenna were measured. The bandwidth and return loss were measured with a vector network analyzer in a normal room. The free-space efficiency and far-field measurements were performed in an echo-free Stargate 24 chamber (Satimo, Villebon-sur-Yvette, France) (Figure 11).

The measurements of the signal strength were performed in a normal room with no shielding from interference and at least 2 m of free space between the user and any other object in the room. The signal-strength measurements were made with three different test scenarios:

- 1) signal strength through 1 m of free space
- 2) signal strength to the front pocket of the user
- 3) signal strength to the back pocket of the user.

RESULTS

Figure 6 shows a detected ECG signal measured with the ECG sensor and sent via the PIFA to the Android application. The readings strongly resemble a normal ECG signal, as shown in Figure 1. The noise in the signal is heavily dependent on the correct placement of the electrodes on the body. The golden standard for ECG measurement is the 12-lead method, using 12 different electrodes to ensure a clear signal

[18]. However, the proposed system utilizes only three electrodes to measure a signal [18], demonstrating that three electrodes are sufficient to produce a satisfactory signal. With the use of more electrodes, a more accurate signal can be produced. However, usability was a priority in designing the BAN, so three electrodes were chosen for simplicity and ease of use.

Table 4 lists the final measurements for the signal strength received by the application. The results are the average value of ten measurements. In the estimated link budgets in Tables 2 and 3, the free-space propagation was estimated to -46.3 dBm, and the creeping-wave propagation was approximated to -66.8 dBm. The measured results were 5.7 and 1.2 dB lower than estimated, respectively.

Figure 12 shows the measured and simulated efficiencies of the antenna. The measured efficiency was lower than the simulated value of 0.82 ; however, it was even over the whole band.

The significant drop in the free-space signal strength can be attributed partially to the simulated free-space efficiency being 1.5 dB higher than the measured efficiency shown in Figure 12 or the possible inaccurate estimation of the receiver gain as -5.3 dBi. The decrease can also be due to the directional nature of the antenna. The system is designed for the antenna to radiate down, toward the user's pocket. This will lead to a decrease in radiation directed forward,

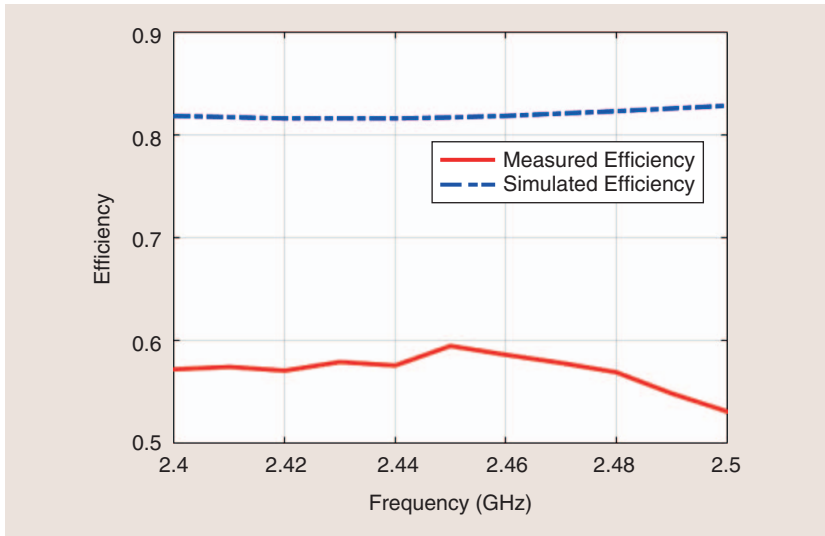


FIGURE 12. The measured and simulated radiation efficiencies of the antenna in free space.

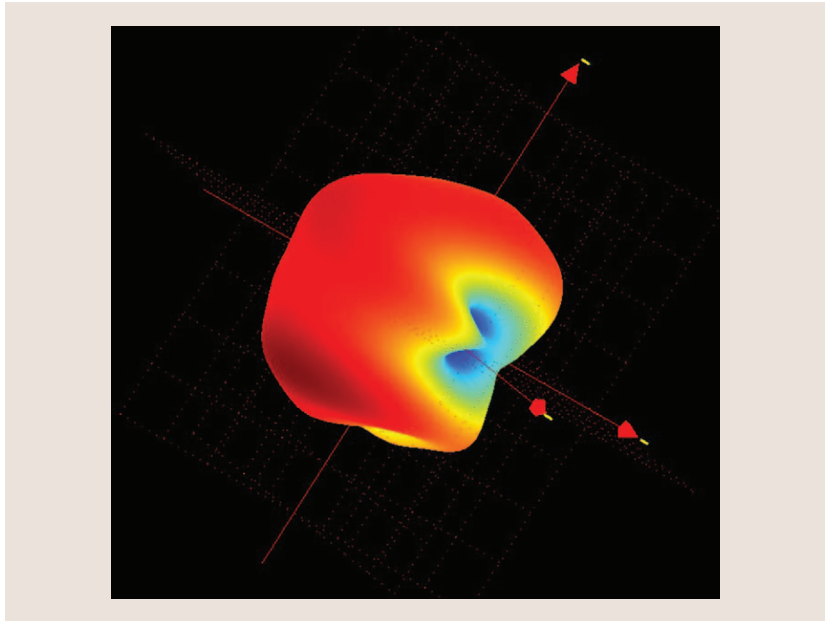


FIGURE 13. The far-field free-space radiation measurement of the antenna at 2.45 GHz. The measurement was performed in the Satimo Stargate 24 measuring chamber at Lite-On Mobile Mechanical in Lund, Sweden. According to the simulations shown in Figure 7, this three-dimensional pattern will be reduced to a hemisphere when placed on a large dielectric load, such as a body.

which was not accounted for in the free-space calculations.

In the creeping-wave estimation, the transmitting and receiving antennas were assumed to be located on either side of the torso. During the back-pocket measurement, the transmitting antenna was located at chest height, whereas the receiving antenna was situated in the back pocket of the user, thus substantially increasing the travel

distance. This increase could account for the lower signal level. However, the received signal is still over the noise floor, and the results are close enough to indicate that the system transmits in the expected way.

The signal strength in the back pocket was significantly lower than the signal strength in the front pocket. There was little difference in free-space distance, and there was no possibility of

the radiation going through the body because, according to the “Simulations and Calculations” section, that would give an ~120-dB lower signal than the free-space signal. This leads to the conclusion that the signal reaching the back pocket could, in part, be of a creeping-wave nature. Furthermore, the radiation lobe of the antenna is heavily biased away from its shorted side (see Figure 7), making creeping-wave propagation more likely.

The far-field measurement in Figure 13 is relatively omnidirectional in one hemisphere. This enables the antenna to radiate to various positions on the body. There is, however, a significant minimum located at the grounded side of the active element. When the system is fastened to the user’s body, the antenna is oriented in such a way as to point this minimum toward the user’s head. Figure 7 shows that the addition of a body bends the far-field radiation pattern toward the user. Thus, the far-field measurement shown in Figure 13 is likely to do the same once the antenna is placed on the body.

The design specifications indicate that prioritized receiving locations are areas used for phone storage, such as pockets or somewhere in the user’s vicinity. The pattern shown in Figure 13 indicates that the antenna might have trouble transmitting to the phone when it is actively used in a phone call or other similar applications. However, because the system is located on the user’s chest, the transmitting distance to the phone during a call will be relatively short and thus not create an issue.

The measured and simulated return losses for free-space and on-body transmissions are plotted in Figure 10. Interestingly, the measured resonances are deeper than the simulated ones. The same behavior is observed in measurements and simulations: when the antenna was placed on the body, the resonance frequency increased slightly and deepened. The effect of the body was not as drastic during measurements as during simulations.

CONCLUSIONS

This article has presented a complete BAN system for the detection of heart

failure using Bluetooth signals with a simple antenna design. Through the use of creeping-wave propagation, the signal can be made to reach locations on the body that are inaccessible without scattering off nearby objects. It has been experimentally shown that this mode of transmission meets the minimum requirement for Bluetooth signals. Thus, any Bluetooth device should be able to maintain contact with the proposed BAN system.

The components used in this prototype are relatively inexpensive, and most are not tailored for measuring ECG signals. Higher-quality hardware and more electrodes would give a clearer and more reliable signal. However, inexpensive manufacturing and ease of use were considerations in the design of this system.

Figure 6 shows that a smartphone's signal processing is enough to measure a recognizable ECG curve. The large percentage of people today who own a smartphone or a similar device ensures that the proposed system can be easily distributed. The cost of the entire system is relatively low, and, by utilizing integrated circuits and a microcontroller tailored for this particular application, the prototype can be made even smaller and more energy efficient. Thus, the system can be mass produced at a low cost and sold separately at a low price to patients and hospitals.

The reliability of correct ECG signals is still an issue for this type of an application. However, this article has demonstrated that it is possible to wirelessly transmit such a signal to commonly available devices. This is a step in the right direction for the future full-time monitoring of high-risk patients. As the signal received in Figure 6 is relatively noise free and shows a clear ST segment, it will be possible to detect an ST elevation with further software development for the prediction of heart attacks.

ACKNOWLEDGMENTS

We thank Anders Sunesson for his expertise and guidance as a mentor and Lite-On Mobile Mechanical for providing their facilities and equipment for radiation measurements. We also thank

Christian Antfolk, Martin Nilsson, Andreas Johansson, Bertil Bengtsson, and Gerhard Kristensson, who all contributed through technical expertise and meaningful advice.

AUTHOR INFORMATION

Georg Wolgast (tna12gwo@student.lu.se) is working toward his M.Sc. degree in engineering, engineering physics, and engineering nanoscience at the Faculty of Engineering, Lund University, Sweden. He is a winner of the 2015 IEEE Antennas and Propagation Society Student Design Contest.

Casimir Ehrenborg (casimir.ehrenborg@eit.lth.se) received his M.Sc. degree in engineering physics from Lund University, Sweden, in 2014. He is currently a Ph.D. student in the Electromagnetic Theory Group, Department of Electrical and Information Technology, Lund University. In 2015, he participated in and won the IEEE Antennas and Propagation Society Student Design Contest for his body area network antenna design. His research interests include stored-energy expression, radiation centers, Q factors, and physical bounds.

Alexander Israelsson (israelsson.alexander@gmail.com) is working toward his M.Sc. degree in engineering and engineering physics at the Faculty of Engineering, Lund University, Sweden. He is a winner of the 2015 IEEE Antennas and Propagation Society Student Design Contest.

Jakob Helander (jakob.helander@eit.lth.se) received his M.Sc. degree in engineering physics from Lund University, Sweden, in 2014. He is currently a Ph.D. student in the Electromagnetic Theory Group, Department of Electrical and Information Technology, Lund University. He was the supervisor for the winning team of the 2015 IEEE Antennas and Propagation Society Student Design Contest. His research interests include computational electromagnetics and antenna design and optimization.

Edvard Johansson (edvard.jo@gmail.com) is working toward his M.Sc. degree in engineering and engineering physics at the Faculty of Engineering,

Lund University, Sweden. He is a winner of the 2015 IEEE Antennas and Propagation Society Student Design Contest.

Hampus Månefjord (hampus.maneffjord@gmail.com) is working toward his M.Sc. degree in engineering and engineering physics at the Faculty of Engineering, Lund University, Sweden. He is a winner of the 2015 IEEE Antennas and Propagation Society Student Design Contest.

REFERENCES

- [1] World Health Organization. (2014, May). The top 10 causes of death. [Online]. Available: <http://www.who.int/mediacentre/factsheets/fs310/en/>
- [2] J. P. Pell, J. M. Sirel, A. K. Marsden, and S. M. Cobbe, "Effect of reducing ambulance response times on deaths from out-of-hospital cardiac arrest: cohort study," *BMJ*, vol. 322, no. 7299, pp. 1385–1388, June 2001.
- [3] P. T. O'Gara, F. G. Kushner, D. D. Ascheim, D. E. Casey, M. K. Chung, J. A. de Lemos, S. M. Ettinger, J. C. Fang, F. M. Fesmire, B. A. Franklin, C. B. Granger, H. M. Krumholz, J. A. Linderbaum, D. A. Morrow, L. K. Newby, J. P. Ornato, N. Ou, M. J. Radford, J. E. Tamis-Holland, C. L. Tommaso, C. M. Tracy, Y. J. Woo, and D. X. Zhao, "2013 ACCF/AHA Guideline for the Management of ST-Elevation Myocardial Infarction: A report of the American College of Cardiology Foundation/American Heart Association Task Force on Practice Guidelines," *Circulation*, vol. 127, no. 4, pp. e362–e425, Jan. 2013.
- [4] E. Burns. (2013). The ST segment. *Life in the Fast Lane*. [Online]. Available: <http://lifeinthefastlane.com/ecg-library/st-segment/>
- [5] eMarketer. (2014, Dec. 11). 2 Billion Consumers Worldwide to Get Smart(phones) by 2016. [Online]. Available: <http://www.emarketer.com/Article/2-Billion-Consumers-Worldwide-Smartphones-by-2016/1011694>
- [6] American Heart Association. (2003, July/Aug.). Anti-clotting agents explained. *Stroke Connection Mag.* [Online]. Available: http://www.strokeassociation.org/STROKEORG/StrokeAfterStroke/HealthyLivingAfterStroke/ManagingMedicines/Anti-Clotting-Agents-Explained_UCM_310452_Article.jsp#.V6I4gxKZP5M
- [7] B. Gulli, *Emergency Care and Transportation of the Sick and Injured*. Boston: Jones & Bartlett, 2009.
- [8] PulsePoint. [Online]. Available: <http://www.pulsepoint.org/>
- [9] M. Raju, *Heart-Rate and EKG Monitor Using the MSP430FG439*. Dallas, TX: Texas Instruments, 2007.
- [10] K. Wong, *Planar Antennas for Wireless Communications*. Hoboken, NJ: Wiley, 2003.
- [11] Henkel. (2010, Oct.). Loctite 431 technical data sheet. [Online]. Available: [https://tds.us.henkel.com/NA/UT/HNAUTTDS.nsf/web/1E919981E9AC68E185257307005F2D07/\\$File/NEW-CA431-EN.pdf](https://tds.us.henkel.com/NA/UT/HNAUTTDS.nsf/web/1E919981E9AC68E185257307005F2D07/$File/NEW-CA431-EN.pdf)
- [12] R. Feick, H. Carrasco, M. Olmos, and H. D. Hristov, "PIFA input bandwidth enhancement by changing feed plate silhouette," *IEEE Electron. Lett.*, vol. 40, no. 15, pp. 921–922, July 2004.
- [13] H. T. Chattha, Y. Huang, and Y. Lu, "PIFA bandwidth enhancement by changing the widths of feed and shorting plates," *IEEE Antennas Wirel. Propagat. Lett.*, vol. 8, pp. 637–640, July 2009.

- [14] T. Alves, B. Poussot, and J.-M. Laheurte, "Analytical propagation modeling of BAN channels based on the creeping-wave theory," *IEEE Trans. Antennas Propagat.*, vol. 59, no. 4, pp. 1269–1274, Apr. 2011.
- [15] R. E. Collin and S. Rothschild, "Evaluation of antenna Q," *IEEE Trans. Antennas Propagat.*, vol. 12, no. 1, pp. 23–27, Jan. 1964.
- [16] Bluetooth. (2014). Bluetooth core specification 4.2. [Online]. Available: <https://www.bluetooth.com/specifications/adopted-specifications>
- [17] J. Tsai, "FCC RF test report FR291007A," Federal Communications Commission, Washington, D.C., Sept. 2012.
- [18] R. Antonicelli, C. Ripa, A. M. Abbatecola, C. A. Capparuccia, L. Ferrara, and L. Spazafumo, "Validation of the 3-lead tele-ECG versus the 12-lead tele-ECG and the conventional 12-lead ECG method in older people," *J. Telemed. Telecare*, vol. 18, no. 2, pp. 104–108, Mar. 2012.

Student and Young Professionals Activities at the 2016 IEEE International Symposium on Antennas and Propagation

The IEEE Antennas and Propagation Society (AP-S) Education Committee sponsors several activities at the Society's annual symposium aimed at students and young

*Digital Object Identifier 10.1109/MAP.2016.2599282
Date of publication: 5 October 2016*

professionals, including the Student Paper Contest, the Student Design Contest, and the Annual Student and Young Professionals Reception.

The Student and Young Professionals Reception this year was a barbecue and beach party on Palomino Island, in San Juan, Puerto Rico. A lively band pulled

the group together for a seemingly magical night of socializing, dancing, and just pure enjoyment of good company on the sand under a beautiful night sky (Figure 1). Many students expressed the hope that the fun and friendly island atmosphere of this year's reception could become an annual tradition.

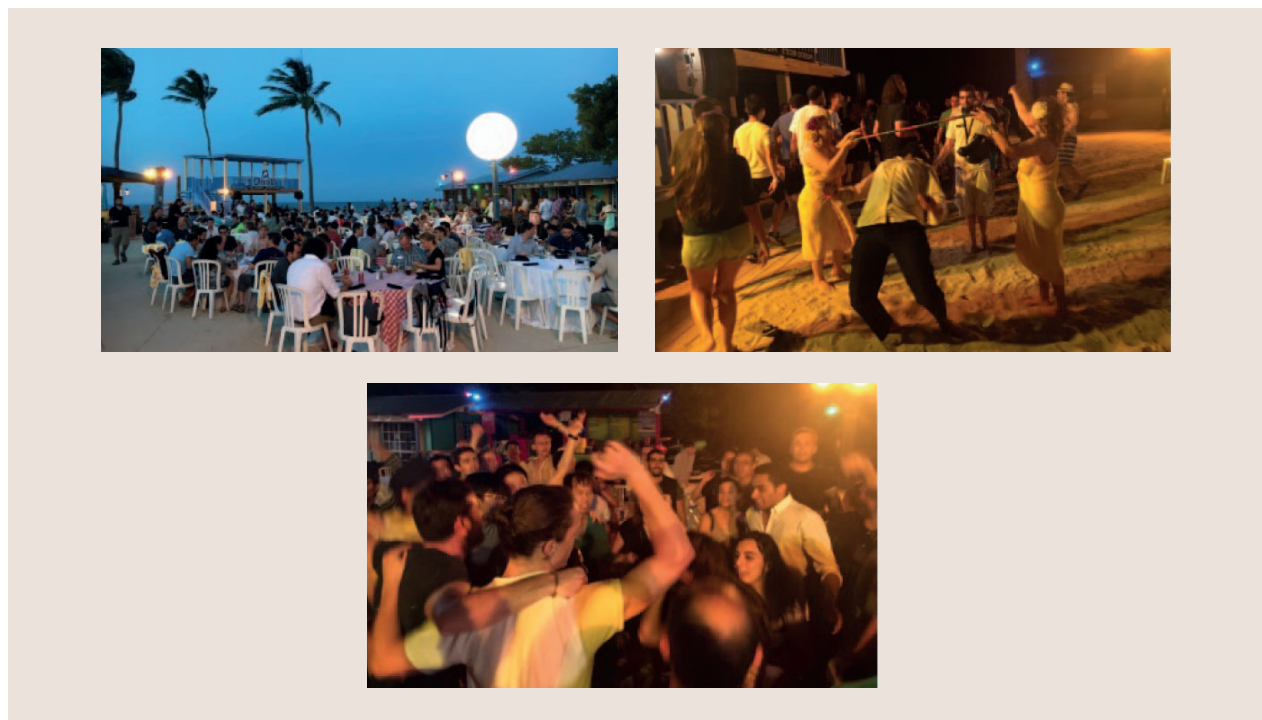


FIGURE 1. Scenes from the 2016 IEEE AP-S Student and Young Professionals Reception in Puerto Rico.